Electrocatalysis of the nitrite reduction : a mechanistic study

Duca, M.

5

Nitrite reduction in alkaline media: a new surface-sensitive probe for the characterization of surfactant-free and colloidal cuboid Pt nanoparticles

Abstract

The "cathodic corrosion" method for nanoparticle synthesis has been used to produce Pt nanoparticles with a preferential "cuboid" shape. Surfactant-free and electrochemically-clean nanoparticles with large percentages of (100) sites have been prepared, and the influence of the pretreatment conditions on the shape of the nanoparticles has been investigated. Classical benchmark electrochemical characterization tests have been performed to establish the amount of (100) sites: blank voltammetry in H_2SO_4, adsorbed CO stripping, Ge irreversible adsorption, and ammonia oxidation. Additionally, nitrite reduction in alkaline media has been proposed as a novel surface-sensitive probe for the characterization of Pt nanoparticles. A comparison to the classical characterization tools has demonstrated that nitrite reduction represents an ancillary, accurate interrogation of the surface structure of Pt nanoparticles with preferential (100) orientation.

An excerpt of this chapter is in preparation for publication.

5.1. Introduction

Supported catalyst nanoparticles are routinely used in many applied catalytic processes[1], enabling the use of expensive active materials dispersed on a large-surface-area support. In the wake of the enormous current interest in nanomaterials, the efficient shape-controlled synthesis of nanoparticles has garnered much attention with a view to large-scale applications of such materials[2]. However, these synthetic routes invariably involve additives or capping agents[3,4] which, despite enabling control over the shape of the growing nanoparticle[5,6], exert a detrimental effect on the catalytic performance of the nanoparticles, acting as surface poisons or modifiers of the catalytic activity[7-9].

In the field of electrocatalysis, where precious metals are often the most active catalysts for many reactions of great importance, the twofold issue of obtaining impurity-free and preferentially-shaped nanoparticles has come to the fore in recent years. The Alicante group has extensively contributed to the research on shape-controlled nanoparticles[10-14], in particular in terms of the development, improvement and standardization of bottom-up synthetic routes, cleaning methods and characterization methods to obtain clean (i.e. free of organic contaminants) nanoparticles for fundamental electrocatalytic studies. Their work has focused on the removal of surface contaminations without the loss of surface order[14] and has mainly involved microemulsion[14] or colloidal[3,15] synthetic routes. As shown by TEM pictures, the fine tuning of these methods enabled the preparation of various controlled shapes: spherical, cubic and cuboctahedral[11]. The *ex-situ* microscopy study was supported by a detailed electrochemical characterization carried out by using blank voltammetry in H_2SO_4 and site-specific surface probes (irreversible adsorption of Bi for the (111) sites[16] and of Ge for the (100) sites[17]). These probes enabled the quantification of the fractions of the various surface sites.

On the contrary, viable surfactant-free preparation protocols for metal nanoparticles were largely unknown until very recently. Huang et al.[18] and Yanson et al.[19] have independently reported on the use of alternating current to disperse a Pt wire in alkaline solutions. The work by Yanson et al., in particular, has focused on the "cathodic corrosion" process, showing the broad potential applicability of this nanoparticle preparation method to most metals and even metal alloys[20]. The use of square-wave potential to induce reorganization of Pt spherical nanoparticles into a tetrahexahedral shape has already been described by Tian et al.[21], and the

effect of electrodeposition potential on the shape of electrodeposited Pt nanoparticles has been recently demonstrated by Hsu et al.[22]; however, to our knowledge there is no previous report on a one-step electrochemical treatment to obtain preferentially-oriented nanoparticles starting from a bulk metal wire.

Preferentially-oriented nanoparticles are crucial to the study of highly structure-sensitive reactions[23]. Nitrite reduction in alkaline media has recently attracted our interest, twenty years after Ye et al.[24] first reported on this subject; their study, focused on Pt basal planes, showed that Pt(100) is by far the most active surface, followed by Pt(110) and Pt(111). Additionally, after the conversion of nitrite to ammonia, Pt(100) was shown to catalyze the re-oxidation of the product to give N_2 [25], in agreement with later reports regarding ammonia oxidation at Pt(100) and vicinal surfaces[26-28]. Our recent work (Chapter 3) reconsidered the properties of a well-ordered Pt(100) electrode for nitrite reduction, focusing on the discovery of an additional reduction peak associated with the direct conversion of NO_2^- to N_2, the latter detected by online mass spectrometry (OLEMS). This new voltammetric feature is extremely sensitive to the quality of the (100) domains, and we have shown that the introduction of controlled defects ("steps") of any symmetry causes a rapid drop in the selective nitrite conversion to N_2 (Chapter 4). The main voltammetric feature (nitrite reduction to ammonia) is also affected by the loss of surface order, although to a lesser extent. Therefore, nitrite reduction in alkaline media is a promising ancillary characterization technique for Pt (cuboid) nanoparticles, being extremely sensitive to the presence of large, well-ordered (100) domains, and we propose it as an alternative or an additional interrogation of the surface structure, along with well-known procedures such as blank voltammetry, Bi and Ge irreversible adsorption[11], CO stripping[12], NH_3 oxidation[13,26-28] and dimethylether (DME) oxidation[29,30], which have all been dealt with in a recent review[23].

The aim of the present chapter is twofold. On the one hand, we demonstrate that the synthesis of extra-clean, preferentially-oriented (cuboid) Pt nanoparticles is feasible by means of cathodic corrosion. On the other hand, we compare these nanoparticles to preferentially-oriented Pt nanoparticles obtained with colloidal synthetic routes in terms of their performance towards well-known benchmark electrochemical tests (ammonia oxidation) and novel surface-sensitive tests (nitrite reduction).

5.2. Experimental

All glassware was cleaned following a standard procedure[31] to remove all traces of organic contaminations. Electrolyte solutions were prepared with Suprapur (Merck) reagents and Millipore MilliQ water (resistivity >18.2 MΩ cm); prior to the experiments oxygen was removed by bubbling argon (purity grade 6.0) through the solution for at least 15 minutes. Argon blanketing was used to protect the solutions during the experiments. $NaNO_2$ (Sigma-Aldrich, 99.999% metal basis) was used as received and then stored in a desiccator under vacuum. All reactants used are of the highest quality available: $(NH_4)_2SO_4$ (Merck, Suprapur®), GeO_2 (Sigma-Aldrich, 99.999% metal basis) and DME(dimethylether) (Sigma-Aldrich, 99.9%).

Surfactant-free Pt cuboid nanoparticles were prepared following a small modification of a published procedure[19]. Typically, a clean Pt wire is subjected to AC cycles (potential extremes -10 and 0 V vs. the graphite counter electrode) in concentrated electrolytes (usually 1 M NaOH), with a frequency of 100 Hz, until a chosen portion of wire has been corroded into metal nanoparticles that precipitate to the bottom of the reaction vessel. Details of the preparations parameters are mentioned in Section 5.3. The cuboid preferential orientation was achieved by repeated and prolonged flame-annealing the Pt wire in a butane/propane flame for at least 15 minutes prior to cathodic corrosion; the importance of controlling the duration of the flame-annealing will be explained in the following section. Before use, the nanoparticle suspension was rinsed with water repeatedly until the pH of the supernatant was approximately neutral; each time, the suspension was centrifuged and the spent supernatant was replaced with a fresh equivalent aliquot. The synthesis and cleaning procedure of colloidal nanoparticles was carried out following a published procedure[11,13].

Prior to the electrochemical studies, a controlled amount of nanoparticles was deposited onto a glassy carbon (GC) or gold working electrode, the latter being chosen for ammonia oxidation, in accordance with previous publications[13]. Both electrodes were polished with alumina suspensions of decreasing sizes to ensure a complete removal of nanoparticles from previous experiments. Alumina particles were removed by sonication in ultrapure water for at least 10 min. The nanoparticle suspension was stirred in an ultrasound bath for 2-3 min. to obtain a homogeneous, well-dispersed suspension and then a droplet (3-4 μl) was deposited onto the

electrode surface. The water was evaporated with a vigorous Ar stream which was flowed over the electrode surface for 5 minutes. The deposition procedure was repeated until a total volume of 8-12 µl (as a function of the nanoparticle concentration in the suspension) was reached. Lower droplet volumes were used for smaller electrodes.

An Autolab PGSTAT20 (bi-)potentiostat was used throughout this work. For all electrochemical experiments involving nanoparticles on glassy carbon, the counter electrode was a platinum flag or wire, which was also flame-annealed and quenched in air. When the surface cleanliness of a gold working electrode was to be checked, a gold counter electrode was used instead. A Reversible Hydrogen Electrode (RHE) was employed as reference electrode for all experiments, and all potentials reported in this chapter are relative to the RHE.

All electrochemical tests of the quality of the surface have been carried out following standard procedures published by other groups[11-13,29,30]. In brief, CO adsorption was carried out at 0.1 V in a 0.5 M H_2SO_4 solution; after vigorous Ar purging of the electrolyte, the CO adlayer was removed with a single positive-going potential excursion (v = 20 mV s^{-1}) with a maximum upper potential limit at 0.87 V to avoid loss of surface order of the nanoparticles. Ge irreversible adsorption was carried out by immersing the nanoparticle-modified electrode in a saturated GeO_2 alkaline solution. The electrode was then transferred to a 0.5 M H_2SO_4 solution protected by a droplet of the GeO_2 solution and immersed under potential control (E = 0.1 V). Repeated scans between 0.1 V and 0.6 V allow one to identify the voltammetric features related to germanium irreversible adsorption. NH_3 oxidation was carried out in a 0.2 M NaOH solution at 10 mV s^{-1} [11].

On-Line Electrochemical Mass Spectrometry (OLEMS) [32] measurements were performed on an EvoLution mass spectrometer system (European Spectrometry Systems Ltd). The system consists of a Prisma QMS200 (Pfeiffer), brought to vacuum with a TMH-071P turbo molecular pump (60 l s^{-1}, Pfeiffer) and a Duo 2.5 rotary vane pump (2.5 m^3 h^{-1}, Pfeiffer). During measurements, the pressure inside the MS was 1 - 5 · 10^{-6} mbar. Additional information can be found in Chapter 2.

5.3. Results and discussion

5.3.1 Nanoparticles prepared with cathodic corrosion.

5.3.1.1 Electrochemical characterization methods: CO_{ads} stripping and Ge irreversible adsorption.

Figure 1 gives an overview of the classical tests used to investigate the quality and the preferential orientations of Pt nanoparticles, applied to a typical batch obtained with cathodic corrosion.

Figure 1A shows the blank voltammetry in 0.5 M H_2SO_4. The hydrogen and anion adsorption/desoprtion on platinum electrodes are well-known fingerprints of the surface sites present on the electrode. It can be seen that three voltammetric features dominate in the blank voltammetry, which can be ascribed to various surface sites[11,23].(110) step sites (also called "defects" later in the text) give rise to the peak at 0.125 V, while the peak at approximately 0.28 V is associated with hydrogen and (bi)sulfate adsorption/desoprtion on short terraces and step sites, both with (100) geometry; if broadened at the bottom, this peak also includes contributions from defects[11]. The wide shoulder at 0.38 V, on the other hand, is a hallmark of larger (100) domains, and more preferentially oriented cubic particles tend to display a small peak on this broad feature[11]. Additionally, the typical voltammetric feature associated with (bi)sulfate adsorption on bidimensionally ordered (111) domains[11] (broad peak located at 0.5 V) is not visible in the voltammogram.

Adsorption of CO and subsequent oxidative "stripping" of this adsorbate mainly serves to remove the remaining trace contaminants; this is harmless for the surface as the blank voltammogram does not change after this treatment. It must be mentioned that CO stripping is not a very site-selective surface probe and its overlap with other processes is still not fully understood. Broadly speaking, the two main peaks, located at 0.71 and 0.767 V, can however be assigned to (111) and (100) sites[12,23,33].

Finally, Figure 1C shows the voltammetric features of the irreversible adsorption of Ge. The full blockage of surface Pt sites is evidenced by the total absence of peaks below 0.3 V; a single, broad oxidation peak is located at around 0.5 V, followed by a reduction peak at 0.39 V in the reverse scan. The charge associated to this process is related to the amount of (100) sites; customarily, only the peak in the positive-going scan is integrated[11].

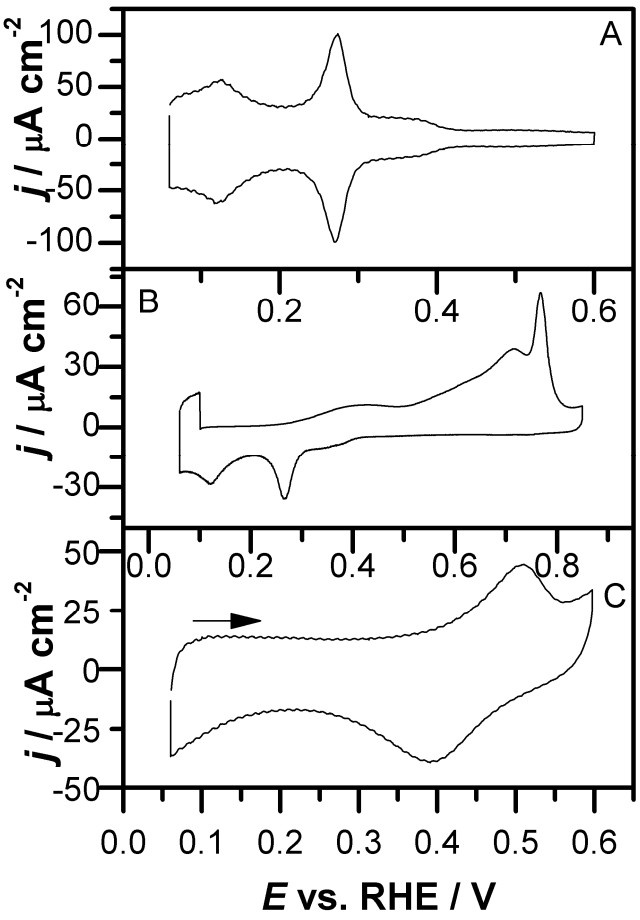

Figure 1 Panel A: blank voltammetric profile (0.5 M H_2SO_4) of nanoparticles obtained with cathodic corrosion and deposited on a gold electrode, v = 50 mV s^{-1}. Panel B: CO stripping for the same nanoparticle batch in 0.5 M H_2SO_4, v = 20 mV s^{-1}. The adsorption was performed in CO-saturated electrolyte while the voltammogram shown was performed after thorough Ar purging (at least 15 min). Panel C: voltammetric features of the irreversible adsorption of Ge at the nanoparticle-modified Au electrode in 0.5 M H_2SO_4, v = 50 mV s s^{-1}. Ge irreversible adsorption indicates a percentage of (100) sites equal to 55%.

All three characterization techniques clearly indicate that the cathodic corrosion technique can produce preferentially-oriented nanoparticles with an absolute majority of (100) surface sites (55%). The blank voltammogram suggests that, due to the absence of the peak related to wide (100) terraces on the broad shoulder at

0.38 V (Figure 1A), most of these (100) sites are narrow terraces, in particular if compared to the cubic colloidal nanoparticles discussed by Solla et al.[11].

Finally, it must be borne in mind that characterization with Ge irreversible adsorption should always be accompanied by the blank voltammetry, because Ge irreversible adsorption occurs at all (100) sites irrespectively of their width[11,17,34]. Thus, only the blank can differentiate between broad and narrow (100) terraces. This piece of information is extremely informative when one investigates reactions preferentially catalyzed by large (100) terraces, such as ammonia oxidation or nitrite reduction (vide infra).

5.3.1.2 Effect of flame-annealing time on the shape of the nanoparticles

The characterization methods described in Section 5.3.1.1 (in particular the blank voltammetry and the Ge irreversible adsorption) allowed us to highlight the paramount importance of the pretreatment of the Pt wire. In particular, a prolonged exposure of the wire to a flame (flame-annealing) is clearly beneficial to the formation of preferentially oriented cuboid nanoparticles with an increase of the percentage of (100) narrow domains and (100) wide terraces. This is shown in Figure 2.

On the shorter timescale, the effect of flame-annealing is not straightforward. The sample that was exposed to the flame for the shortest span of time (thick line, Figure 2) features a sharp peak associated with narrow (100) domains but also a rather large peak of defects at lower potentials (the ratio between these two peak currents, r_{blank}, is equal to 1.3), and the feature related to (100) large terraces is almost completely absent. A hardly visible enlargement around 0.5 V evidences that (111) facets, if present, are small and practically negligible. Ge irreversible adsorption indicates that 31 % of the surface sites are oriented as (100). An increase of the flame-annealing time brings about a minor increase of the percentage of the (100) sites to reach 35% (dotted line, Figure 2); the blank voltammetry shows that the ratio between narrow (100) domains and defects is slightly improved (r_{blank} =1.4) although the broadening of the voltammetric peak located at 0.27 V suggests that the width of the narrow (100) terraces has decreased. The feature related to wide (100) terraces has however grown. The most well-oriented cuboid nanoparticles are obtained with prolonged annealing (thin line). The percentage of (100) sites reaches 55 %; the peak associated with narrow

(100) domains grows and become sharper, while the presence of defect sites further decreases, r_{blank} being equal to 1.8. Finally, the blank voltammetric feature of (111) sites is completely absent.

Thus, we can conclude that the optimal preparation of preferentially-oriented cuboid nanoparticle involves a prolonged exposure of the Pt wire to the flame prior to cathodic corrosion. The effect of the flame temperature also plays an important role. Preliminary experiments shown that higher temperatures of annealing (before the melting point) improve the formation of cubic nanoparticles. It must also be noted that, apparently, our preparation procedure avoids the formation of (111) domains.

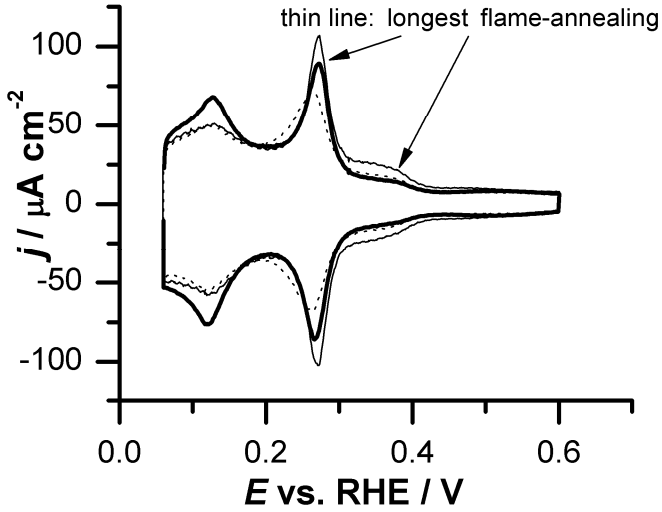

Figure 2 Blank voltammetric profile (0.5 M H_2SO_4) of nanoparticles obtained with cathodic corrosion and deposited on a gold electrode, v = 50 mV s^{-1}. The annealing time is equivalent to: 5 repetitions of heating/cooling for a total time of 5 min in the flame (thick line); 5 repetitions of heating/cooling for a total time of 8 min in the flame (dotted line); 2 repetitions of heating/cooling for a total time of 15 min in the flame (thin line). The sample shown as a thin line is the same shown in Figure 1. All nanoparticles are prepared in 1 M NaOH.

5.3.1.3 Nitrite reduction in alkaline media as a characterization tool.

The reduction of nitrite ions in 0.1 M NaOH is a strongly surface-sensitive electrochemical reaction that can successfully be employed to characterize platinum nanoparticles, as mentioned in the Introduction.

Figure 3 compares nitrite reduction at Pt single crystal electrodes to the voltammetric profile obtained with Pt cuboid nanoparticles. The first reduction peak at E = 0.18 V compares well with the main nitrite reduction peaks at (110) electrodes, and so it can be assigned to nitrite reduction at "defect" sites. The large reduction peak at ca. 0.35 V and the small feature at 0.58 V arise from nitrite reduction (to NH_3) at (100) domains. Thus, the two latter peaks can be used as a straightforward indication of the "cubicalness" of the Pt cuboid nanoparticles. The oxidation signal recorded at 0.65 V, also associated with Pt(100) electrodes (see Chapter 4), could be used as further indication of the presence of well-ordered (100) facets. Additionally, further evidence of the structure sensitivity of nitrite reduction in alkaline media can be gained by directly comparing the blank voltammogram of Pt cuboid nanoparticles to the corresponding voltammetric profiles during nitrite reduction. Figure 4 shows such comparison for the nanoparticle samples with most and least (100) sites from Figure 2.

The blank voltammogram in H_2SO_4 lets us appreciate the difference between the two samples, as already discussed above (Figure 3). Not surprisingly, the sample with the higher percentage of (100) sites and the largest peak of broad (100) terraces in the blank voltammogram is also more performing with respect to nitrite reduction, although both batches display a certain amount of defects (peak at 0.18 V in Figure 4B). This is evidenced by the appearance of a more prominent reduction peak at 0.35 V in Figure 4B characteristic of nitrite reduction to ammonia at (100) domains. Additionally, the sample represented with a thin line shows a much larger peak (at 0.58 V in Figure 4B) related to the direct conversion of nitrite to N_2, along with the oxidative feature during the positive-going scan (peak at 0.5 V, Figure 4B) typical of ammonia oxidation at well-ordered, large (100) domains. Figure 4 therefore demonstrates that the study of the voltammetric features of nitrite reduction can corroborate the information obtained by the blank voltammetry in sulfuric acid, being able to address in a single experiment defect sites, (100) narrow and broad terraces. In these terms, nitrite reduction is an ancillary probe, along with blank voltammetry and Ge irreversible adsorption, to estimate the width of the (100) domains. In this regard, the ratio between the current densities of the (100) sites at 0.35 V and the "defect" peak at 0.18 V, which

we shall call $\rho_{nitrite}$, can be compared to r_{blank}, introduced in the previous section. Figure 5 shows that $\rho_{nitrite}$ increases approximately with a linear fashion as a function of r_{blank}; each of the two parameters can thus be independently used to express the amount of (100) domains with respect to other surface sites. This is an expected results, because both $\rho_{nitrite}$ and r_{blank} contain, by definition, parameters related to identical surface sites (defects and (100) –narrow- terraces). Clearly, the presence of the peak associated with N_2 evolution is a more direct evidence of the presence of broad (100) terraces and indicates, as suggested by our previous report (Chapter 4), that (100) terraces broader than four atoms are present on the nanoparticle surface.

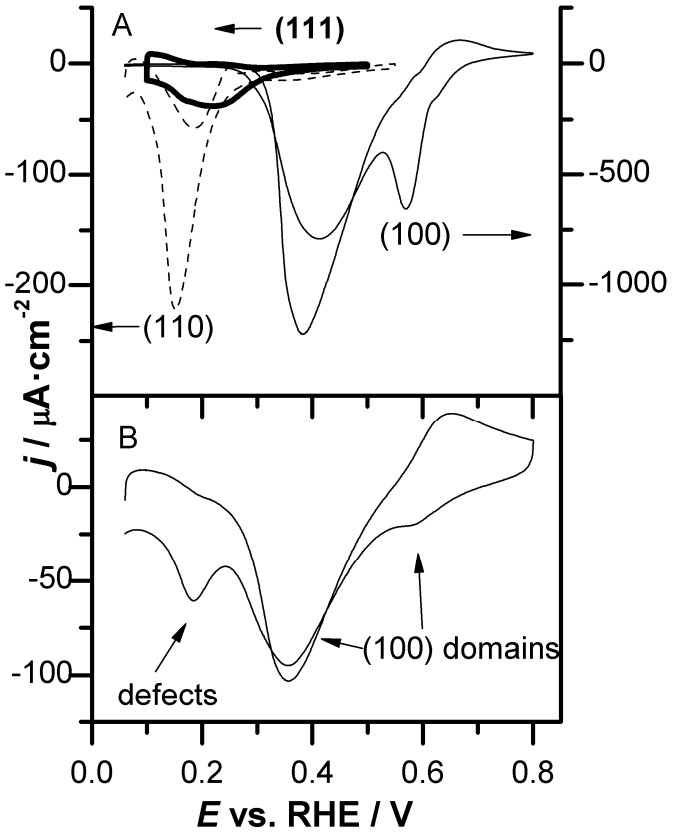

Figure 3 Panel A: Synopsis of the voltammetric profiles for the continuous reduction of 2 mM $NaNO_2$ on the three basal planes in 0.1 M NaOH. Thin line Pt(100), dashed line Pt (110), thick line Pt (111), v = 20 mV s^{-1}. Panel B: Voltammetric profile for the continuous

reduction of 2 mM $NaNO_2$ at a batch of Pt cuboid nanoparticles in 0.1 M NaOH. The amount of (100) sites of the nanoparticles used was 59 % (determined with the Ge irreversible adsorption). For details on the peak labels, see text.

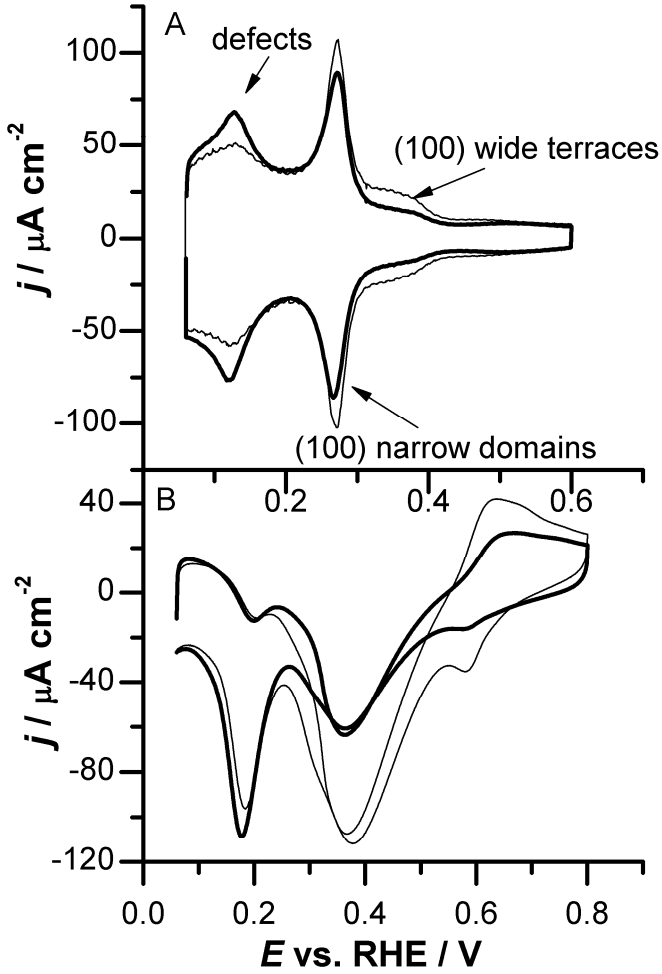

Figure 4 Panel A: Blank voltammetric profile (0.5 M H_2SO_4) of nanoparticles obtained with cathodic corrosion and deposited on a gold electrode, v = 50 mV s^{-1}. The annealing time is equivalent to: 5 repetitions of heating/cooling for a total time of 5 min in the flame (thick line); 2 repetitions of heating/cooling for a total time of 15 min in the flame (thin line). The percentage of (100) sites (calculated with Ge irreversible adsorption) is 31% (thick line) and 55% (thin line). Panel B: voltammetric profiles for the reduction of 2 mM $NaNO_2$ in 0.1 M NaOH, v = 20 mV s^{-1}. Thick and thin lines as in panel A.

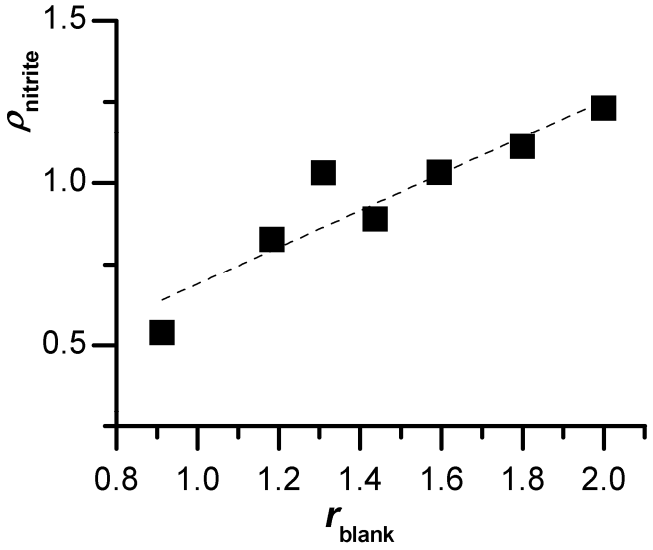

Figure 5 Graphical representation of the relationship between $\rho_{nitrite}$ and r_{blank}, two parameters both proportional to the amount of (100) sites on the nanoparticle. $\rho_{nitrite}$ is defined as $\rho_{nitrite} = j_{(100)peak} / j_{defects}$ during nitrite reduction, while $r_{blank} = j_{(100)narrow\ terrace\ peak} / j_{(110)peak}$ in the blank voltammogram in 0.5 M H_2SO_4.

The structure sensitivity of nitrite reduction in NaOH can also highlight the effects of aging on the performances and the quality of the nanoparticles; in fact, if a surfactant-free nanoparticle suspension is stored for several months after preparation, a decrease of its preferential orientation can be detected. This is shown in Figure 6, where the voltammetric profile of nitrite reduction (of the same batch used in Figure 1) is recorded again five months after preparation.

The detrimental effect of aging is already evident when the voltammetric profiles in the blank electrolyte are compared. The aged sample shows loss of charge for the peak associated with the short (100) domains and a growth of the peak of the defect sites. A minor loss of charge for the shoulder signal associated with wide (100) domains can also be noticed. The study of nitrite reduction further evidences the disordering of the surface structure due to aging. The large reduction peak centered at around 0.35 V shows a threefold decrease while the peak characteristic of nitrite reduction at defect sites is doubled. However, the voltammetric feature signaling direct nitrite conversion to N_2 is still appreciable, while the aging-induced decrease of the oxidative feature is also evident. The disordering of the cuboid

nanoparticles is not surprising, since the (111) orientation is the most thermodynamically stable surface; thus, (100) sites should slowly convert into (111).

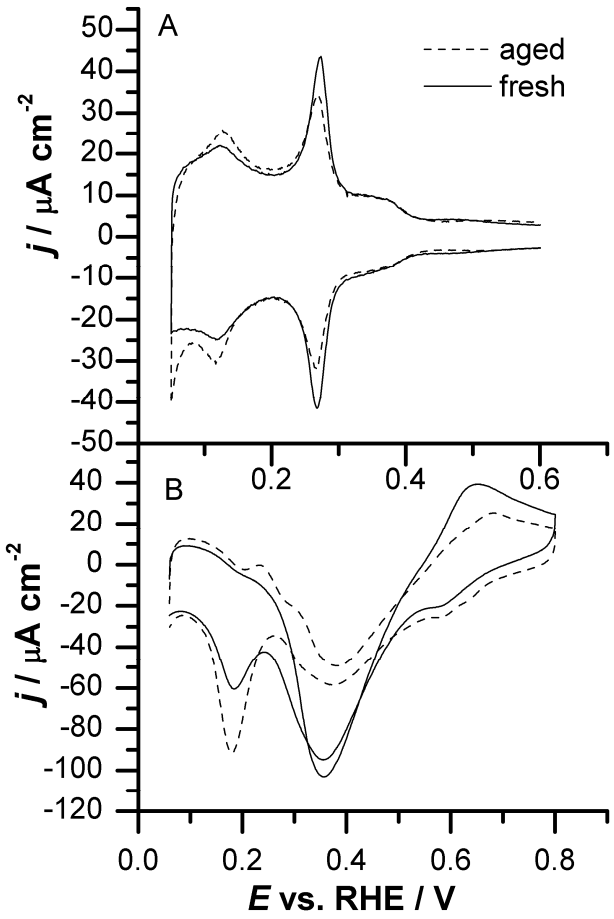

Figure 6 Panel A: the effect of aging on the blank voltammogram on cuboid Pt nanoparticles, electrolyte 0.5 M H_2SO_4, v = 20 mV s^{-1}. Panel B: the effect of aging on the voltammetric features of nitrite reduction on cuboid Pt nanoparticles in 0.1 M NaOH, v = 20 mV s^{-1}. The amount of (100) sites of the fresh nanoparticles was 59 % (determined with the Ge irreversible adsorption[11]).

The freshly-prepared nanoparticles were also tested for N_2 evolution in the OLEMS setup in a similar experiment as those of Chapters 3 and 4. Figures 7 and 8 show the voltammetric profiles, along with the recorded ion current traces for *m*/*z* 14 (N)

and *m/z* 28 (N_2). The small voltammetric peak at 0.59 V is associated with the evolution of N_2 in both scan directions. The amount of N_2 generated is appreciable, because it is also possible to detect the nitrogen fragment *m*/*z* 14, which accounts for 10% of the intensity of the *m*/*z* 28 signal[35].

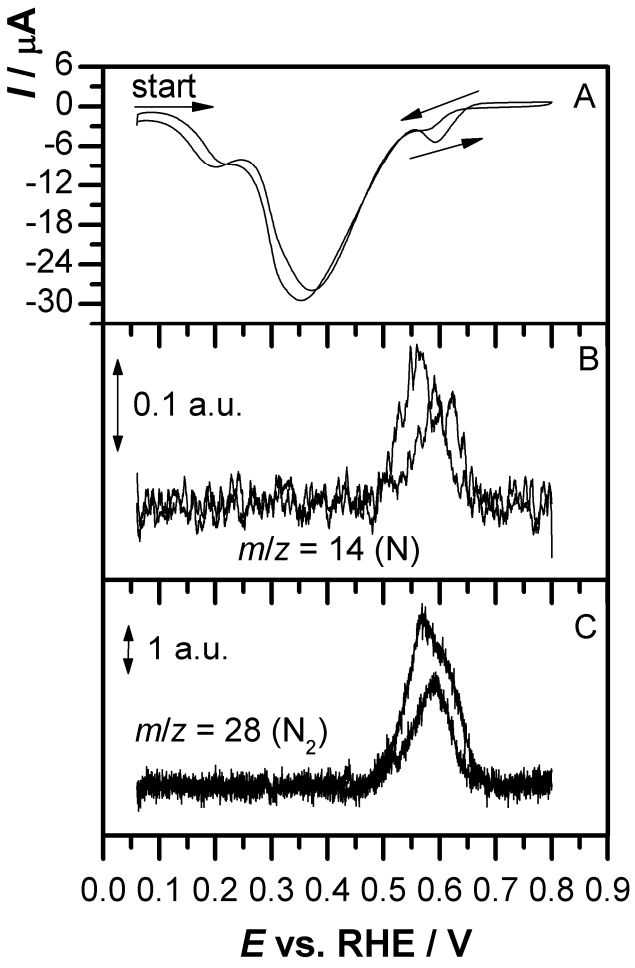

Figure 7 Panel A: Cyclic voltammetry during OLEMS measurements at a nanoparticle-modified pyrolytic graphite electrode and ion current profiles for *m/z* = 14 (Panel B) and *m/z* = 28 (Panel C) in 0.1 M NaOH containing 2 mM $NaNO_2$, v = 1 mV s^{-1}. The arrows indicate the direction of the potential sweep. The amount of (100) sites of the nanoparticles is 59 % (determined with the Ge irreversible adsorption).

The quality of the (100) is crucial to the selective nitrite conversion to N_2. If the preferentially oriented (100) sites decrease, in fact, the amount of N_2 produced drops very quickly (Chapter 4). This is shown in Figure 8, where a nanoparticle batch with a lower percentage of (100) sites yields much less N_2 (and, as a consequence, *m*/*z* 14 cannot be detected), which is just produced during the positive-going sweep. The voltammetric profile also indicates minor nitrogen formation: the peak at 0.59 V can barely be noticed.

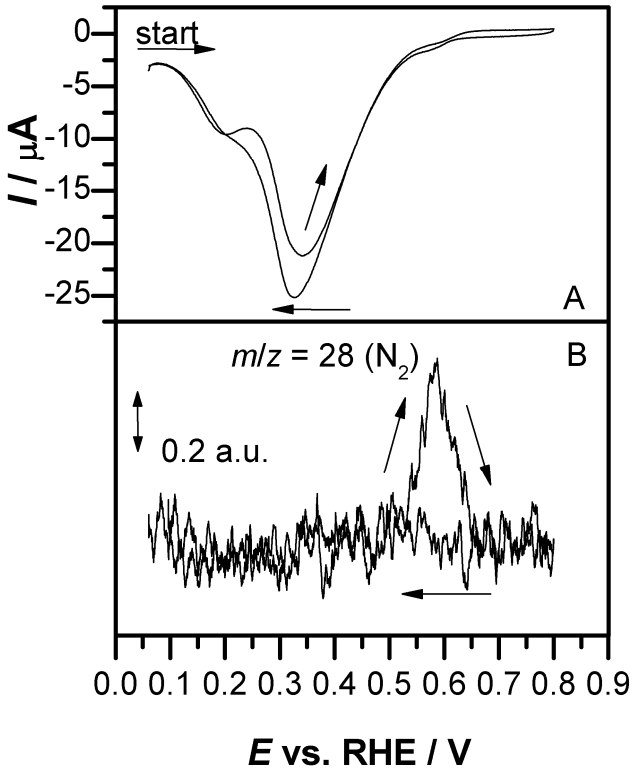

Figure 8 Panel A: Cyclic voltammetry during OLEMS measurements at a nanoparticle-modified pyrolytic graphite electrode and ion current profiles for *m/z* = 28 (Panel B) in 0.1 M NaOH containing 2 mM $NaNO_2$, v = 1 mV s^{-1}. The arrows indicate the direction of the potential sweep. The amount of (100) sites of the nanoparticles is 51 % (determined with the Ge irreversible adsorption).

5.3.1.4 Ammonia oxidation

Ammonia oxidation is commonly used as a benchmark for the presence of well-ordered (100) on Pt nanoparticles[13,23]. Studies on Pt single-crystals have shown that the ammonia oxidation activity rapidly decreases with increasing step density for Pt(S)[*n*(100) × (111)] or Pt(S)[*n*(100) × (110)] stepped surfaces[27]. The highest current density for the oxidation of 0.1 M NH_3 in 0.2 M NaOH on Pt cubic nanoparticles, equal to 1350 μA cm^{-2}, has been reported by the Alicante group[13]. In order to do a proper comparison, we performed our experiments under identical conditions.

Figure 9 shows the catalytic activity of the nanoparticles samples prepared by the cathodic corrosion method towards the ammonia oxidation in alkaline media, along with their blank cyclic voltammetry profiles in 0.5 M H_2SO_4.

Sample 1 shows a very broad and intense voltammetric feature at 0.7 V and the higher catalytic activity toward the ammonia oxidation 1110 μA cm^{-2} which is characteristic of larger well-ordered (100) domains. The comparison with the least active sample (4, dotted line) highlights the paramount importance of long-range, ordered (100) domains in the oxidation of ammonia. The almost total absence of large (100) terraces in the blank voltammetry of batch 4 (panel B) brings about a dramatic drop in the electrocatalytic activity towards ammonia oxidation along with a much later onset potential of the oxidation. Batch 4 is the worst even though 31 % of the sites are oriented as (100) because it mainly features narrow (100) terraces. So, short (100) terraces (highlighted by the peak at approximately 0.28 V in Figure 9B) seem to play a secondary role for this reaction: for instance, samples 1 and 4 feature a similar amount of short (100) domains. The comparison between samples 2 and 3 leads to similar conclusions. Therefore, the trends for ammonia oxidation corroborate the results of the tests based on other characterization methods, demonstrating at the same time that we can prepare cuboid nanoparticles with a remarkable ammonia oxidation activity.

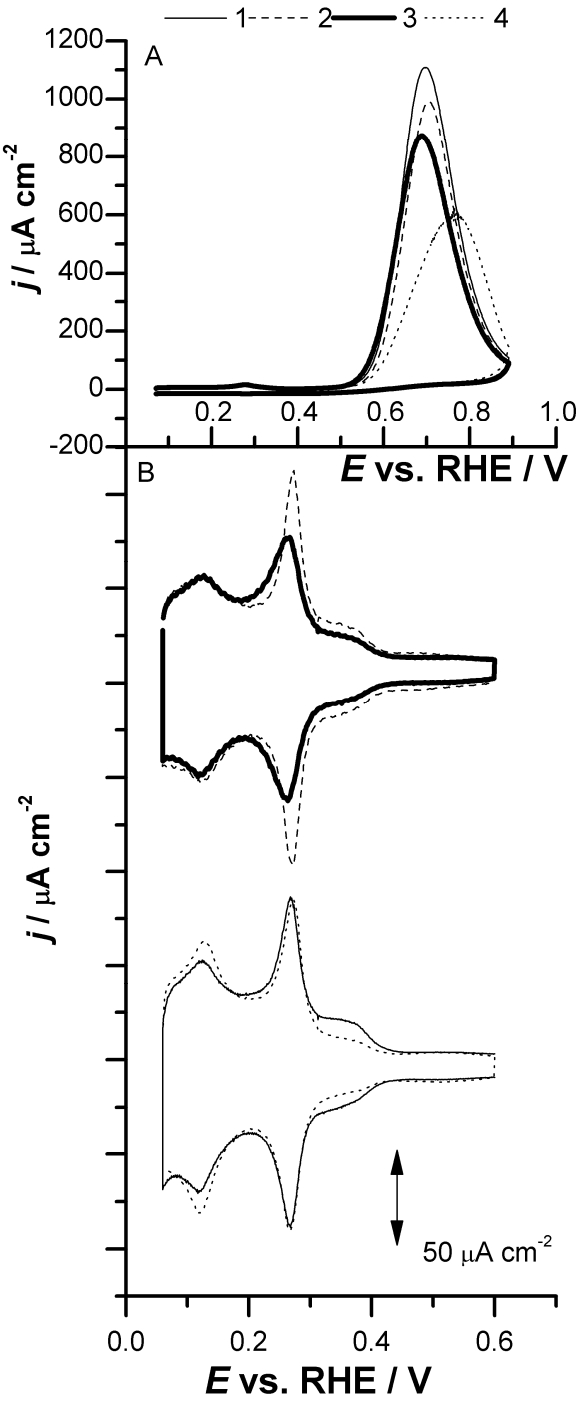
1
2
3
4
A
B
j / μA cm-2
E vs. RHE / V
50 μA cm-2

Figure 9 Panel A: Electrocatalytic activity towards ammonia oxidation for four nanoparticle samples prepared with cathodic corrosion. The reaction was carried out in a 0.2 M NaOH solution containing 0.1 M NH_3, v = 10 mV s^{-1}. Percentage of (100) sites measured with Ge irreversible adsorption: 59 % (sample 1), 55% (sample 2), 35 % (sample 3), 31 % (sample 4). Panel B: a comparison of the blank voltammograms for the four samples in 0.5 M H_2SO_4, v = 50 mV s^{-1}.

5.3.1.5 DME oxidation

The oxidation of DME (dimethylether) (saturated solution in 0.5 M H_2SO_4) has recently been proposed as another site-selective probe for the evaluation of (100) domains[23,29,30]. Figure 10 displays the first two voltammetric cycles for the oxidation of DME at preferentially-oriented cuboid nanoparticles (the same sample as in Figure 1, with 55% (100) sites).

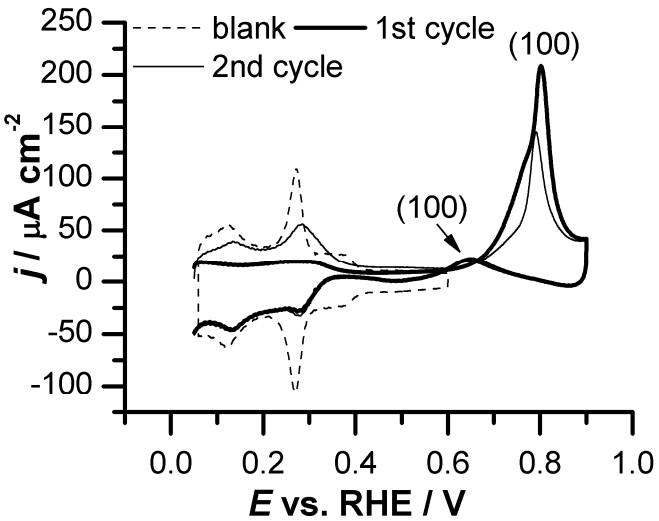

Figure 10 Electrocatalytic activity towards DME oxidation for nanoparticles prepare with cathodic corrosion. The reaction was carried out in a DME-saturated 0.5 M H_2SO_4 solution containing, v = 50 mV s^{-1}. Pt nanoparticles were deposited on a GC electrode.

The voltammetric profiles in Figure 10 feature a large oxidation peak (centered at 0.8 V) in the positive-going scan. This peak is typically associated with (100) domains and corroborates the results obtained with other characterization methods throughout this chapter. A second, smaller oxidation feature in the negative-going

sweep is also indicative of well-ordered (100) peaks, as shown in Figure 10. It is important to note that there are a few discrepancies with published results. In particular, the intensity of the peak currents decreases in the second cycle, in disagreement with the report by Lu et al.[30]; additionally, another large oxidation peak was observed in the first cycle at 0.25 V, which we did not detect. Since we followed the procedure described by Lu et al[30], we tend to ascribe these discrepancies to the accumulation of small amounts of contaminations at the Pt nanoparticles upon cycling. In fact, Lu et al[30] performed their experiments with 99.99 % DME (supplied by Sumitomo), while we performed our experiments with 99.9 % DME (Sigma-Aldrich) which, to our knowledge, is the highest quality DME currently available on the market.

5.3.2 Nitrite reduction as a tool for characterization of colloidal nanoparticles.

Nitrite reduction was also used to investigate the surface preferential orientation for colloidal nanoparticles. Figure 11, panels A and C, show the blank voltammetric profile of two samples of colloidal nanoparticles.

The blank voltammetry in Figure 11A is distinctive of "cuboctahedral" (or "truncated octahedral") nanoparticles[13], featuring large, well-oriented (111) sites, associated with the voltammetric signal at 0.5 V typical of sulfate/bisulfate adsorption[11], along with the voltammetric peaks characteristic of narrow and long (100) sites. It can be seen (Figure 11B) that nitrite reduction is able to "deconvolute" the complexity of the nanoparticle surface, highlighting the contribution of every site to this reaction. Specifically, the presence of large and well-ordered (111) domains give rise to the shoulder at 0.27 V in Figure 11B, merged with the broader main peak, which can be associated with nitrite reduction at (111) terraces, as demonstrated by previous experiments with single-crystals[24] (see Figure 1, and Chapters 3 and 4). The main peak, typical of nitrite reduction to ammonia at (100) sites, evidences the presence of a certain percentage of (100) sites. On the other hand, the small peak associated with N_2 evolution signals that these nanoparticles also feature large (100) facets, corroborating the evidence of the blank voltammetry (Figure 11A). Figure 10C shows a second batch prepared following a colloidal synthetic route: in this case, the blank voltammetry displays most of the features also visible in Figure 11A but the peak associated with (100) narrow terraces has a larger relative magnitude (with respect to the (110) peak, which is less sharp than in Figure 11A) and the (111) (bi)sulfate adsorption feature

is weaker. Nitrite reduction can effectively highlight these peculiarities: the shoulder related to nitrite reduction at (111) sites is very weak and barely appreciable in Figure 11D, while the peaks related to (100) domains and defects predominate in the voltammogram

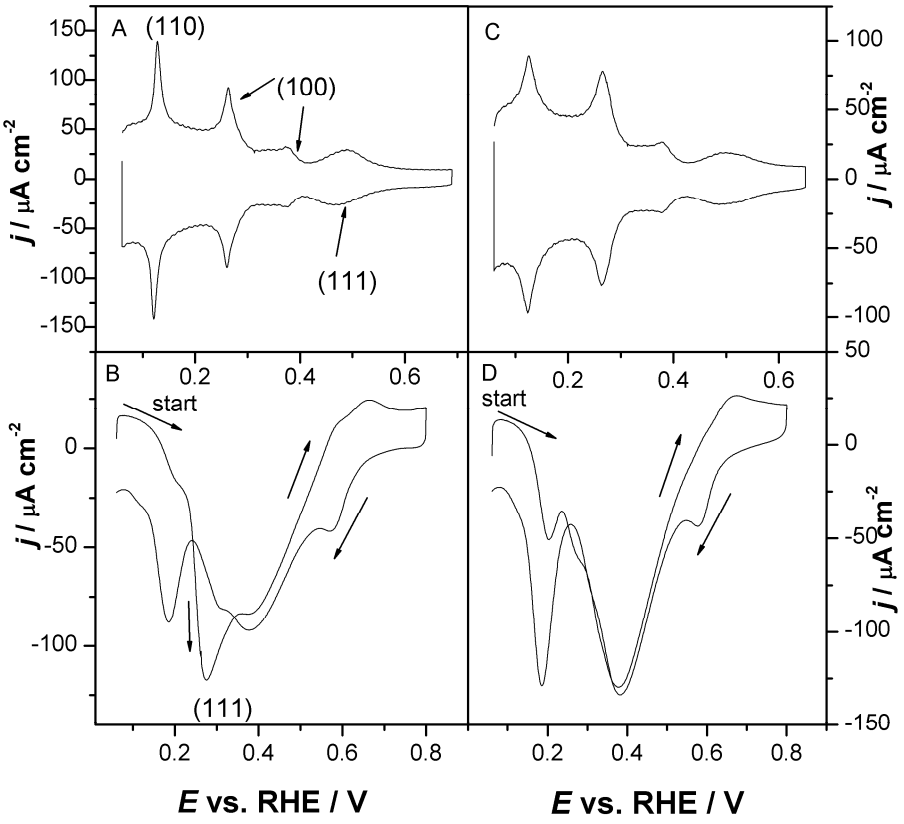

Figure 11 Panels A and C: blank voltammograms for the four batches in 0.5 M H_2SO_4 of two nanoparticle samples prepared with the colloidal method, v = 50 mV s^{-1}. Panels B and D: voltammetric profiles for the reduction of 2 mM $NaNO_2$ in 0.1 M NaOH, v = 20 mV s^{-1}. Panels A-B and C-D refer to the same nanoparticle sample.

.5.3.3. Cleanliness of cathodic corrosion particles

In this final subsection we will show that the cleanliness level of cathodic corrosion particles is superior to that of nanoparticles prepared with the colloidal synthetic route. This is particularly important in that even the most benign cleaning

procedures may eventually harm the preferentially-oriented surface structure of the nanoparticle; additionally, cleaning steps are often tedious.

Figure 12 clearly shows that the typical cleaning methods used for Pt nanoparticles (which also correspond to the characterization methods discussed in Section 5.3.1.1: adsorbed CO stripping and irreversible Ge adsorption) do not improve the surface cleanliness of nanoparticles obtained with cathodic corrosion (Figure 12A). In other words, the hydrogen adsorption region is not affected by the cleaning procedure. On the other hand, CO adsorption and Ge irreversible adsorption can dramatically improve the level of cleanliness of nanoparticles prepared with the colloidal synthesis, as shown in Figure 12B. The effect of Ge, in particular, is remarkable: it is particularly effective in removing "contamination" from broad (100) terraces.

5.4. Conclusions.

We have demonstrated that the cathodic corrosion method can successfully be applied to the preparation of preferentially-shaped Pt nanoparticles, producing "cuboid" nanoparticles with a percentage of (100) sites as high as 59%. With respect to cuboid nanoparticles prepared with the so-called colloidal method, nanoparticles synthesized with "cathodic corrosion" feature a superior cleanliness level and a negligible presence of large (111) terraces. The latter piece of information seems to indicate that cathodic corrosion cannot easily generate such domains. The amount of (100) domains can be enhanced by accurately controlling the parameters of the pretreatment, specifically the duration of the flame-annealing of the Pt wire prior to cathodic corrosion.

Nitrite reduction in alkaline media, which is known to be a highly surface-sensitive reaction, can be employed as ancillary characterization tool for Pt nanoparticles featuring a preferential (100) orientation. In particular, the ratio of the voltammetric peaks associated with (100) and defects sites is a direct indicator of the quality of the surface orientation of the nanoparticles. Unlike Ge irreversible adsorption and ammonia oxidation, nitrite reduction can highlight all surface sites in a single experiment, similarly to a blank voltammogram. Finally, nanoparticles with large (100) terraces display the voltammetric peak typical of direct nitrite conversion to N_2, and this gas can successfully be detected with the OLEMS setup.

This suggests that cubic or cuboid nanoparticles could be promising practical catalysts in the field of wastewater remediation.

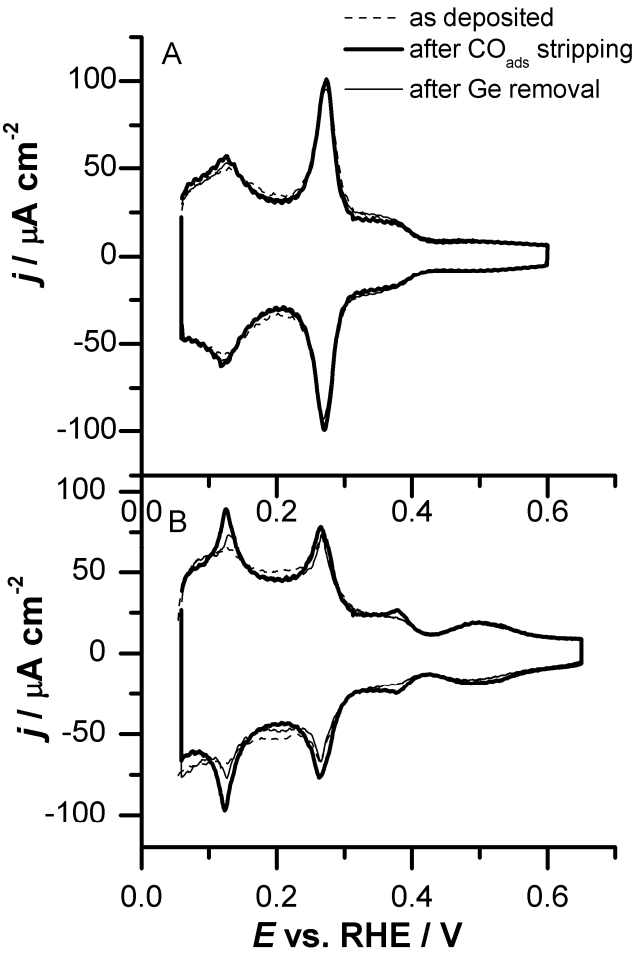

Figure 12 Panel A: blank voltammograms in 0.5 M H_2SO_4 for a typical nanoparticle batch prepared with cathodic corrosion, after treatment with CO and Ge, v = 50 mV s^{-1}. Panel B: blank voltammograms in 0.5 M H_2SO_4 for a typical nanoparticle batch prepared with colloidal synthesis, after treatment with CO and Ge, v = 50 mV s^{-1}

5.5. Acknowledgements

We acknowledge partial financial support from the European Commission (through FP7 Initial Training Network "ELCAT", Grant Agreement No. 214936-2).

M.T.M.K. acknowledges financial support from The Netherlands Organization for Scientific Research (NWO-Middelgroot) for the purchase and development of the online electrochemical mass spectrometer. Lastly, we also gratefully acknowledge a NWO for a VIDI scholarship.

Appendix – Supporting Information

Cathodic corrosion in 10 M NaOH

Figure A1 displays the voltammetric features for hydrogen adsorption and nitrite reductions for two nanoparticle samples synthesized in 10 M NaOH with two different potential programs.

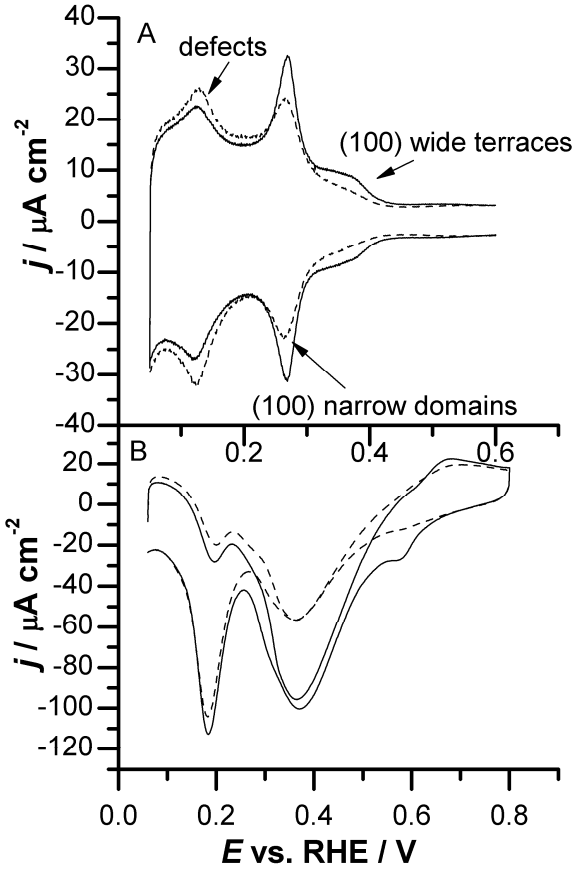

Figure S1 Panel A: Voltammetric profile of Pt nanoparticles in 0.5 M H_2SO_4, v = 20 mV s^{-1}. Dotted line: nanoparticles prepared with AC cycles between -5 and 0 V (vs. GC counter electrode), υ = 100 Hz, electrolyte 10 M NaOH . Continuous line: nanoparticles prepared with AC cycles between -10 and 0 V (vs. GC counter electrode), υ = 100 Hz, electrolyte 10 M NaOH. Panel B: voltammetric profiles for the reduction of 2 mM $NaNO_2$ in 0.1 M NaOH, v = 20 mV s^{-1}. Dotted and continuous lines as in panel A.

References

(1) Raimondi, F.; Scherer, G. G.; Kotz, R.; Wokaun, A. *Angew. Chem.-Int. Edit.* **2005**, *44*, 2190-2209.
(2) Li, Y. M.; Somorjai, G. A. *Nano Lett.* **2010**, *10*, 2289-2295.
(3) Ahmadi, T. S.; Wang, Z. L.; Green, T. C.; Henglein, A.; ElSayed, M. A. *Science* **1996**, *272*, 1924-1926.
(4) Yang, J.; Ying, J. Y. *Nat. Mater.* **2009**, *8*, 683-689.
(5) Tao, A. R.; Habas, S.; Yang, P. D. *Small* **2008**, *4*, 310-325.
(6) Xia, Y. N.; Xiong, Y. J.; Lim, B.; Skrabalak, S. E. *Angew. Chem.-Int. Edit.* **2009**, *48*, 60-103.
(7) Kuhn, J. N.; Tsung, C. K.; Huang, W.; Somorjai, G. A. *J. Catal.* **2009**, *265*, 209-215.
(8) Park, J. Y.; Aliaga, C.; Renzas, J. R.; Lee, H.; Somorjai, G. A. *Catal. Lett.* **2009**, *129*, 1-6.
(9) Kim, C.; Lee, H. *Catal. Commun.* **2009**, *10*, 1305-1309.
(10) Vidal-Iglesias, F. J.; Solla-Gullon, J.; Herrero, E.; Montiel, V.; Aldaz, A.; Feliu, J. M. *Electrochem. Commun.* **2011**, *13*, 502-505.
(11) Solla-Gullon, J.; Rodriguez, P.; Herrero, E.; Aldaz, A.; Feliu, J. M. *Phys. Chem. Chem. Phys.* **2008**, *10*, 1359-1373.
(12) Solla-Gullon, J.; Vidal-Iglesias, F. J.; Herrero, E.; Feliu, J. M.; Aldaz, A. *Electrochem. Commun.* **2006**, *8*, 189-194.
(13) Vidal-Iglesias, F. J.; Solla-Gullon, J.; Rodriguez, P.; Herrero, E.; Montiel, V.; Feliu, J. M.; Aldaz, A. *Electrochem. Commun.* **2004**, *6*, 1080-1084.
(14) Solla-Gullon, J.; Montiel, V.; Aldaz, A.; Clavilier, J. *J. Electroanal. Chem.* **2000**, *491*, 69-77.
(15) Ahmadi, T. S.; Wang, Z. L.; Henglein, A.; ElSayed, M. A. *Chem. Mater.* **1996**, *8*, 1161-&.
(16) Clavilier, J.; Feliu, J. M.; Aldaz, A. *J. Electroanal. Chem.* **1988**, *243*, 419-433.
(17) Rodriguez, P.; Herrero, E.; Solla-Gullon, J.; Vidal-Iglesias, E. J.; Aldaz, A.; Feliu, J. M. *Electrochim. Acta* **2005**, *50*, 3111-3121.
(18) Huang, W.; Chen, S.; Zheng, J. F.; Li, Z. L. *Electrochem. Commun.* **2009**, *11*, 469-472.
(19) Yanson, A. I.; Rodriguez, P.; Garcia-Araez, N.; Mom, R. V.; Tichelaar, F. D.; Koper, M. T. M. *Angew. Chem. Int. Ed.* **2011**, *50*, 6346-6350.
(20) Rodriguez, P.; Tichelaar, F. D.; Koper, M. T. M.; Yanson, A. I. *J. Am. Chem. Soc.* **2011**, *article ASAP*.
(21) Tian, N.; Zhou, Z. Y.; Sun, S. G.; Ding, Y.; Wang, Z. L. *Science* **2007**, *316*, 732-735.
(22) Hsu, I. J.; Esposito, D. V.; Mahoney, E. G.; Black, A.; Chen, J. G. G. *J. Power Sources* **2011**, *196*, 8307-8312.

(23) Koper, M. T. M. *Nanoscale* **2011**, *3*, 2054-2073.
(24) Ye, S.; Hattori, H.; Kita, H. *Ber. Bunsen-Ges. Phys. Chem.* **1992**, *96*, 1884-1886.
(25) Gao, Y. Z.; Kita, H.; Hattori, H. *Chem. Lett.* **1994**, 2093-2096.
(26) Vidal-Iglesias, F. J.; Solla-Gullon, J.; Feliu, J. M.; Baltruschat, H.; Aldaz, A. *J. Electroanal. Chem.* **2006**, *588*, 331-338.
(27) Vidal-Iglesias, F. J.; Solla-Gullon, J.; Montiel, V.; Feliu, J. M.; Aldaz, A. *J. Phys. Chem. B* **2005**, *109*, 12914-12919.
(28) Vidal-Iglesias, F. J.; Garcia-Araez, N.; Montiel, V.; Feliu, J. M.; Aldaz, A. *Electrochem. Commun.* **2003**, *5*, 22-26.
(29) Lu, L. L.; Yin, G. P.; Tong, Y. J.; Zhang, Y.; Gao, Y. Z.; Osawa, M.; Ye, S. *J. Electroanal. Chem.* **2010**, *642*, 82-91.
(30) Lu, L. L.; Yin, G. P.; Wang, Z. B.; Gao, Y. Z. *Electrochem. Commun.* **2009**, *11*, 1596-1598.
(31) Lai, S. C. S.; Koper, M. T. M. *Faraday Discuss.* **2009**, *140*, 399-416.
(32) Wonders, A. H.; Housmans, T. H. M.; Rosca, V.; Koper, M. T. M. *J. Appl. Electrochem.* **2006**, *36*, 1215-1221.
(33) Kinge, S.; Urgeghe, C.; De Battisti, A.; Bonnemann, H. *Appl. Organomet. Chem.* **2008**, *22*, 49-54.
(34) Gomez, R.; Llorca, M. J.; Feliu, J. M.; Aldaz, A. *J. Electroanal. Chem.* **1992**, *340*, 349-355.
(35) *NIST Chemistry WebBook, NIST Standard Reference Database Number 69*; Linstrom, P. J.; Mallard, W. G., Eds. Gaithersburg MD, 20899, http://webbook.nist.gov, retrieved February 18, 2010.